

Short Communication

A wall-mounted source array for the excitation of incoherent broadband sound fields with prescribed modal distributions in ducts

Wontae Jeong^{a,*}, Soogab Lee^b, P. Joseph^c

^a*Technical Research Institute, Hyundai Mobis, Gyenggi-do 80-10, Korea*

^b*Center for Environmental Noise and Vibration Research, School of Mechanical & Aerospace, Seoul National University, Seoul 151-744, Korea*

^c*Institute of Sound and Vibration Research, University of Southampton, Highfield, Southampton SO17 1BJ, UK*

Received 29 November 2004; accepted 10 December 2004

Available online 8 November 2005

Abstract

In the analysis of broadband sound fields in ducts, for example, turbofan engines, large exhaust stacks, and exhaust mufflers, the assumption of ‘Equal Energy per Mode’ (EEpM) is frequently made. The practical realization of such a sound field is valuable as a means of, for example, allowing liner attenuation measurements obtained from measurements on different test rigs to be compared directly, or for allowing measurement results to be compared with computer predictions in which the assumption is made. This paper describes a technique in which arrays of sound sources at the wall of a duct are driven by white noise signals to generate a sound field of prescribed modal energy distribution and modal coherence. The number of sources required for effective mode synthesis and the source geometry are also discussed. An example is presented in which ‘EEpM’ broadband sound field is generated up to a maximum non-dimensional frequency of $ka = 20$ using 152 sources.

© 2005 Elsevier Ltd. All rights reserved.

1. Introduction

There are many situations in which it is desirable to be able to generate a broadband sound field within a duct of known modal content. The availability of a standardized in-duct sound field is useful as a means of, for example, allowing the multi-mode performance of different liners or duct silencers obtained from different tests to be compared directly, or for allowing measurement results to be meaningfully compared with computer predictions. Presently, there are no guidelines for the definition of such a sound field. However, in many analyses of broadband sound fields in ducts, the assumption of ‘Equal Energy per Mode’ (hereafter termed EEpM,) is frequently made [1–4]. Here the sound field in a narrow frequency is assumed to comprise all propagating modes with equal energy and their mode amplitudes are uncorrelated [1–4]. Another reason for the usefulness of the EEpM sound field is indicated in the recent work of Joseph and Morfey [4], who have

*Corresponding author. Tel.: 822 880 7382; fax: 822 887 2662.

E-mail address: wontae@snu.ac.kr (W. Jeong).

shown that in this sound field there is a simple and well-behaved relationship between the in-duct acoustic pressure and the sound power. This is not the case in, for example, the sound field due to a distribution of monopoles. This relationship allows the sound power flowing along the duct to be readily determined from comparatively few measurements of acoustic pressure.

Whilst in-duct testing with an EEPM sound field is desirable for the reason stated above, the facilities required to generate such a sound field is currently very costly. One way of approximating an EEPM sound field is by locating one end of the duct in a large reverberation chamber at high frequency, thereby exciting the duct with an approximately diffuse sound field.

This paper is concerned with an alternative approach for generating an EEPM broadband sound field with uncorrelated mode amplitudes. The procedure uses sound sources on the duct wall driven by a white noise signal passing through a matrix of shaping filters. Inverse methods are used to calculate the cross-spectra of the strengths of sources arranged in a number of rings mounted on the duct wall for exciting an EEPM sound field in a hard-walled circular duct. Note that the effects of reflections and flow are neglected in this paper, although they are readily incorporated within the theory. Optimal number of sources are investigated and the distance between source rings is evaluated for generating a broadband sound field with incoherent modal amplitude.

2. Theory of broadband sound field generation in ducts

2.1. Duct mode theory

At a single frequency ω , an incident mode propagating along the duct shown in Fig. 1 without reflection, can be written in the form

$$p_{mn}^+ = e^{j\omega t} a_{mn} \Psi_{mn}(r, \phi) e^{-j\alpha_{mn}kz}, \tag{1}$$

where a_{mn} is the mode amplitude, k is the free space wavenumber ω/c , and c is the sound speed in the duct.

The term (m, n) denotes the usual circumferential and radial mode indices. Here κ_{mn} are a set of eigenvalues that are characteristic of the duct cross-section, which satisfies the hard-walled boundary condition $J'(\kappa_{mn}a) = 0$, where J_m denotes the Bessel function of the first kind of order m , the prime signifies differentiation with respect to the argument, and a is the duct radius. The term α_{mn} is the non-dimensional axial wavenumber $\alpha_{mn} = \sqrt{1 - (\kappa_{mn}/k)^2}$, which takes values between $\alpha = 0$ at the modal cut-off frequency, $\omega = \omega_{mn} = \kappa_{mn}c$, and $\alpha = 1$ as $\omega/\omega_{mn} \rightarrow \infty$, corresponding to modes well above cut-on. The term $\Psi_{mn}(r, \phi)$ is the normalized mode shape function, which in a hard-walled circular duct is given by

$$\Psi_{mn} = J_m(\kappa_{mn}r) e^{jm\phi} / N_{mn}, \tag{2}$$

where N_{mn} is chosen to satisfy the mode normalization condition $S^{-1} \int_S |\Psi_{mn}|^2 dS = 1$, where S is the duct cross-sectional area.

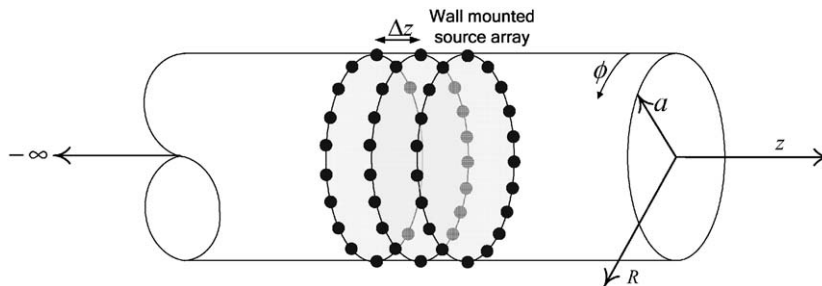


Fig. 1. The source array is comprised of a number of rings, N_r with a distance between them of Δz . Each ring contains a certain number of sources, $N_{s/r}$ and the sources are mounted on the duct wall. Sources are driven to construct predefined sound field.

The time-averaged sound power $\overline{W}^+(ka)$ flowing along the duct is given by

$$\overline{W}^+ = \text{Re} \left\{ \frac{i}{2\omega\rho} \int_S d\mathbf{x} p^+ * (\mathbf{x}) \frac{\partial p^+(\mathbf{x})}{\partial z} \right\}, \quad \mathbf{x} \in S, \tag{3}$$

where ρ is the ambient fluid density. Substituting Eq. (1) into Eq. (3) and performing the integration by the orthogonal property of the mode shape function gives

$$\overline{W}_{mn} = \frac{S}{2\rho c} \sum_{m,n} E\{|a_{mn}|^2\} \alpha_{mn} (\alpha_{mn} : \text{real}), \tag{4}$$

where \overline{W}_{mn} is time-averaged sound power of mode of the (m, n) th and the modal summation is taken only over the propagating modes, $(\alpha_{mn} : \text{real})$. If the sound power in each of the incident modes at a single frequency are assumed to be ϖ , and the mode amplitudes assumed to be uncorrelated (we treat the mode amplitude as random variables), from Eq. (4) this gives

$$\left. \begin{aligned} E\{|a_{mn}|^2\} &= \frac{2\rho c\varpi}{S} \alpha_{mn}^{-1}, & (m, n) &= (m', n') \\ E\{a_{mn}a_{m'n'}^*\} &= 0, & (m, n) &\neq (m', n') \end{aligned} \right\}. \tag{5}$$

In the broadband problem, we wish to compute the optimal source strength time series $q_i(t)$ with frequency spectrum $q_i(\omega)$, where $q_i(t)$ is the i th time record with duration T . The cross-spectral matrix S_{qq} is given by

$$S_{qq} = \lim_{T \rightarrow \infty} E \left\{ \frac{1}{T} \mathbf{q} \mathbf{q}^H \right\} = \lim_{T \rightarrow \infty} \begin{pmatrix} E \left\{ \frac{1}{T} |q_1|^2 \right\} & E \left\{ \frac{1}{T} \{q_1 q_2^*\} \right\} & \cdots & E \left\{ \frac{1}{T} \{q_1 q_l^*\} \right\} \\ E \left\{ \frac{1}{T} \{q_2 q_1^*\} \right\} & E \left\{ \frac{1}{T} |q_2|^2 \right\} & \cdots & \cdot \\ \cdot & \cdot & \ddots & \cdot \\ E \left\{ \frac{1}{T} \{q_l q_2^*\} \right\} & \cdot & \cdots & E \left\{ \frac{1}{T} |q_l|^2 \right\} \end{pmatrix} \tag{6}$$

which excites, in a least-squares sense, a mode amplitude distribution whose cross-spectral matrix, from Eq. (5), is given by

$$S_{aa} = \lim_{T \rightarrow \infty} E \left\{ \frac{1}{T} \mathbf{a} \mathbf{a}^H \right\} = \frac{2\rho c\varpi}{S} \begin{pmatrix} \alpha_1^{-1} & 0 & 0 & \cdots & 0 \\ 0 & \alpha_2^{-1} & \cdot & \cdot & 0 \\ \cdot & \cdot & \alpha_k^{-1} & \cdot & \cdot \\ \cdot & \cdot & \cdot & \cdot & \cdot \\ 0 & \cdot & \cdot & \cdot & \alpha_K^{-1} \end{pmatrix}, \tag{7}$$

where $k = (m, n)$, K is the number of propagating modes and ‘ H ’ denotes the Hermitian transpose operator.

2.2. Optimal source strength spectral matrix

The vector of mode amplitudes $\hat{\mathbf{a}}_i^T = [a_{1i}(\omega) \ a_{2i}(\omega) \ a_{3i}(\omega) \ \dots \ a_{Ni}(\omega)]$ excited by the source array with source strengths $\hat{\mathbf{q}}_i^T = [q_{1i}(\omega) \ q_{2i}(\omega) \ q_{3i}(\omega) \ \dots \ q_{Ni}(\omega)]$ may be written in terms of a modal coupling matrix \mathbf{G} :

$$\hat{\mathbf{a}}_i = \mathbf{G} \hat{\mathbf{q}}_i + \mathbf{e} \tag{8}$$

whose (k, l) th term relates to the coupling between the k th source and the mode amplitude of the l th mode. This term may be written as $G_{kl} = \Psi_l(r_k, \phi_k) e^{-i\alpha_l k z_k} / (2\rho c \alpha_l)$. The optimal estimate of $\hat{\mathbf{q}}_{i0}$ that minimizes the

sum of squared errors $\mathbf{e}^H \mathbf{e} = (\mathbf{a} - \hat{\mathbf{a}})^H (\mathbf{a} - \hat{\mathbf{a}})$ is given by

$$\hat{\mathbf{q}}_{io} = \mathbf{G}^+ \mathbf{a}_i, \tag{9}$$

where \mathbf{G}^+ denotes the pseudo-inverses of \mathbf{G} and $\mathbf{G}^+ = [\mathbf{G}^H \mathbf{G}]^{-1} \mathbf{G}^H$ for the case where there are more sources than modes (the over-determined case). The corresponding optimal source-strength cross-spectral matrix is defined by

$$\mathbf{S}_{qqo} = \lim_{T \rightarrow \infty} E \left\{ \frac{1}{T} \hat{\mathbf{q}}_{io} \hat{\mathbf{q}}_{io}^H \right\}. \tag{10}$$

Substituting Eq. (9) into Eq. (10) gives the optimal source-strength cross-spectral matrix as

$$\mathbf{S}_{qqo} = \mathbf{G}^+ \mathbf{S}_{aa} \mathbf{G}^{+H} \tag{11}$$

from which the least-squares best estimate for the mode-amplitude cross-spectral matrix can be written as

$$\hat{\mathbf{S}}_{aa} = \mathbf{G} \mathbf{S}_{qqo} \mathbf{G}^H. \tag{12}$$

2.3. Realization of optimal shaping filters

Eq. (12) specifies the optimum cross-spectral source matrix, which excites, in the least-squares sense, an EEpM sound field with incoherent mode amplitudes. It provides no guidelines as to how these L^2 source strength cross-spectra may be realized in practice. We now investigate the design of an array of filters which can be used to excite a loudspeaker array at the duct wall to generate a broadband sound field in the duct which has equal energy in a narrow frequency band.

We assume that the source strengths can be generated by a square matrix of shaping filters \mathbf{H} , driven by a number of input signals $\mathbf{x}^T = [x_1(\omega) \quad x_2(\omega) \quad \cdots \quad x_N(\omega)]$,

$$\mathbf{q}_{so} = \mathbf{H} \mathbf{x}. \tag{13a}$$

A schematic diagram of this process is shown in Fig. 2.

The i th source strength produced by the sum of N optimally weighted input signals is therefore

$$q_{i,so}(\omega) = H_{i,1}(\omega)x_1(\omega) + H_{i,2}(\omega)x_2(\omega) + \cdots + H_{i,N}(\omega)x_N(\omega). \tag{13b}$$

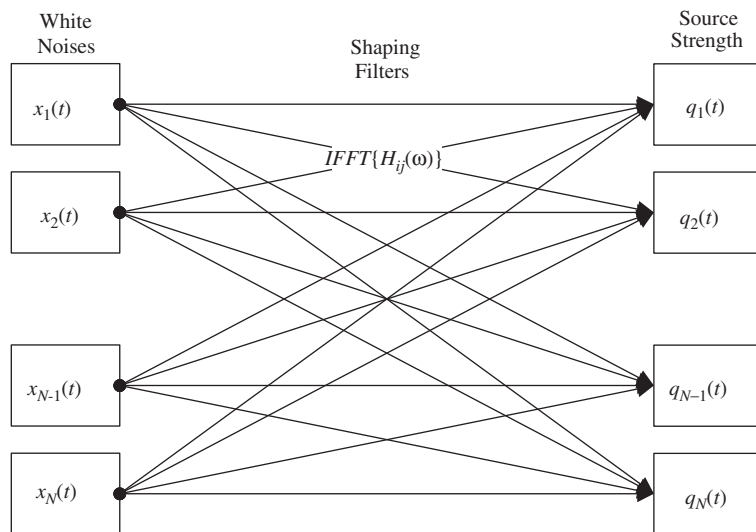


Fig. 2. Schematic diagram of the generating process of generating an EEpM broadband sound field with shaping filters and white noise input signals.

The optimal source cross-spectral matrix is therefore given by

$$\mathbf{S}_{qqo} = \mathbf{H}\mathbf{S}_{xx}\mathbf{H}^H, \tag{14}$$

where $\mathbf{S}_{xx} = (\pi/T)E\{\mathbf{x}\mathbf{x}^H\}$. For simplicity, but without loss of generality, we assume that the vector of input signals \mathbf{x} comprises uncorrelated white noise signals so that

$$\mathbf{S}_{xx} = \sigma^2\mathbf{I}, \tag{15}$$

where \mathbf{I} is the identity matrix and σ^2 is the mean square value of the noise signal \mathbf{x} . The cross-spectral source strength matrix \mathbf{S}_{qqo} becomes

$$\frac{\mathbf{S}_{qqo}}{\sigma^2} = \mathbf{H}\mathbf{H}^H. \tag{16}$$

Since the cross-spectral matrix \mathbf{S}_{qqo} is Hermitian, i.e., $\mathbf{S}_{qqo} = \mathbf{S}_{qqo}^H$, it can be expressed in terms of its eigenvector and eigenvalue matrices \mathbf{U} and $\mathbf{\Sigma}$, respectively, in the form

$$\frac{\mathbf{S}_{qqo}}{\sigma^2} = \mathbf{U}\mathbf{\Sigma}\mathbf{U}^H. \tag{17}$$

Comparing with Eq. (16) indicates that matrix of shaping filters \mathbf{H} may be related directly to \mathbf{U} and $\mathbf{\Sigma}$ by

$$\mathbf{H} = \mathbf{U}\mathbf{\Sigma}^{1/2}. \tag{18}$$

3. Example results and discussion

A typical result of the broadband mode synthesizer is shown in Fig. 3. It shows the modal power plotted against cut-on ratio α_{mn} at $ka = 15$ generated by seven rings of sources, each containing 19 sources. The upper figure is a plot of modal power versus cut-on ratio α_{mn} , where positive and negative α -values are used to distinguish modes with $+m$ and $-m$ values. The lower figure shows the modal coherence, defined by $E\{|a_{mn}a_{m'n'}^*|^2\}/[E\{|a_{mn}|^2\}E\{|a_{m'n'}|^2\}]$. We now consider the number and arrangement of sources needed to ensure accurate mode synthesis.

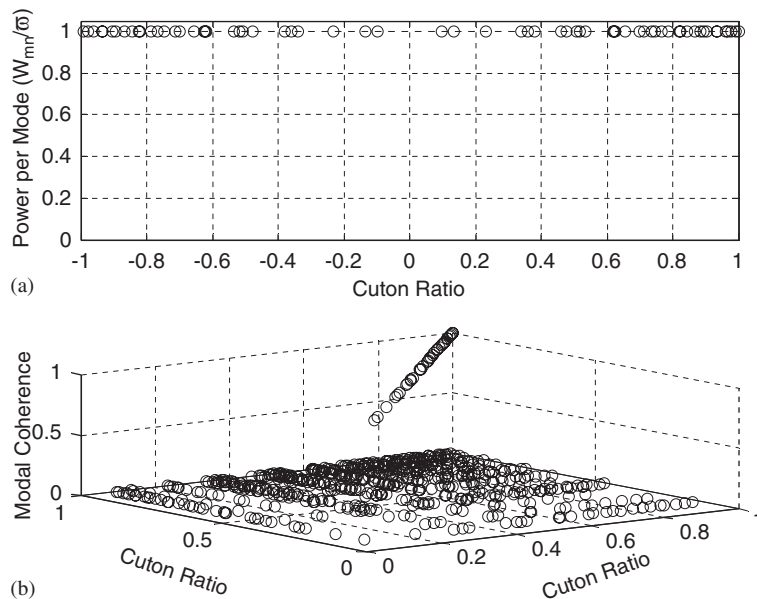


Fig. 3. Typical result of the broadband synthesis at $ka = 20$ using seven rings of sources, each containing 19 sources. (a) Modal energy versus α_{mn} . (b) Modal coherence versus α_{mn} .

3.1. Number of optimal sources and source geometry

Consider the sources to be arranged on the wall of the duct, as shown in Fig. 1, in N_r rings, separated by distance Δz , each ring comprising $N_{s/r}$ sources. For broadband sound fields excited over a limited frequency range, the number of optimal sources required for accurate sound field synthesis is investigated. The number of propagating modes increases approximately as the frequency is squared. The number of sources required for accurate reconstruction of the sound field also increases with the same power law. In this paper, we set the criteria for satisfactory mode synthesis as the deviation between modal energies and mutual modal coherence as being better than 10%, i.e.,

$$|W_{mn}/\varpi - 1| < 0.1, \quad \gamma_{mm'n'}^2 = \frac{E\{|a_{mn}a_{m'n'}^*\|^2\}}{E\{|a_{mn}|^2\}E\{|a_{m'n'}|^2\}} < 0.1. \quad (19a,b)$$

For a given ka , all source rings are separated by a distance of $\lambda/2$. The minimum N_{tot} satisfying the criterion of Eq. (19) is chosen as the optimal configuration of source rings and sources per rings obtained by a searching algorithm which finds the minimum N_{tot} value by varying $N_{s/r}$ and N_r . The optimal values of $N_{s/r}$ and N_r against non-dimensional frequency ka are plotted in Fig. 4.

From Fig. 4(a), $N_{s/r}$ is always an odd number and less than $2m_{max} + 1$, which is the number of spinning modes. Note that the optimal value of N_r is slightly greater than, or equal to, the maximum radial mode order n_{max} (associated with $m = 0$). The total number of sources, $N_{tot} = N_{s/r}N_r$ required for accurate mode synthesis can be seen to be slightly greater than the number of possible propagating modes. Although a change in source geometry could reduce the number of optimal sources required, considering the criteria of Eq. (19) suggests that the total number of modes is equal to the lower limit of N_{tot} .

Considering the sampling theorem in relation to the excitation of circumferential modes by the source rings will be shown to be useful in understanding why the optimal value of $N_{s/r}$ is odd and less than $2m_{max} + 1$. The volume velocity variation along the duct wall can be expressed as sum of modal components

$$q(\varphi) = \sum_{m=-\infty}^{\infty} q_m \Psi_m(\phi). \quad (20)$$

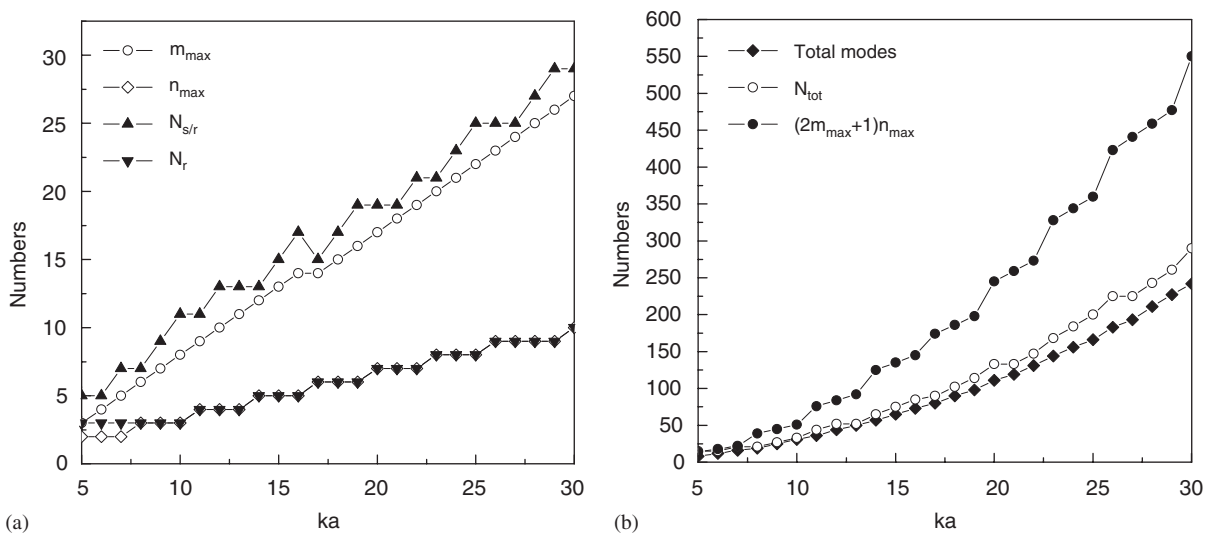


Fig. 4. Number of sources to construct EEPm sound field, which satisfy criteria of power and coherence. Both graphs compare the number of sources with number of modes. (a) Optimum number of sources per ring and number of source rings. (b) Optimum number of total sources.

The *ortho*-normal property of mode shape functions allows the m_1 th harmonic component of source strength to be written as

$$q_{m_1} = \int q(\phi) \Psi_{m_1}^* dS. \quad (21)$$

For a single source ring with sources separated in angle by $2\pi/N_{s/r}$, substituting Eq. (2) into Eq. (21) gives

$$q_{m_1} = \sum_{n=0}^{N_{s/r}-1} \frac{J_{m_1}(\kappa_m a)}{N_{m_1}} q(\varphi_n) e^{-j(2\pi/N_{s/r})m_1 n} \quad (22)$$

In Eq. (22), the term $e^{-j(2\pi/N_{s/r})m_1 n}$ plays an important role in determining the amplitude of each mode independently. If two modes m_1 and m_2 give identical values of $e^{-j(2\pi/N_{s/r})m_1 n}$ and $e^{-j(2\pi/N_{s/r})m_2 n}$, the two modes cannot be generated independently by a given source distribution $q(\varphi_n)$. In this case, the value of $(2\pi/N_{s/r})m_1 - (2\pi/N_{s/r})m_2$ must be multiples of 2π , for example, $m_1 - m_2 = N_{s/r}$. If there are two modes which satisfy $m_1 - m_2 = N_{s/r} + n$ (where n is positive integer, not a multiple of $N_{s/r}$ or zero) then two modes can be generated independently. Numbers of sources per ring $N_{s/r}$ greater or equal to $2m_{\max} + 1$, therefore, prevent aliasing between two spinning modes, because of the property, $m_1 - m_2 \leq |m_1| + |m_2| < 2m_{\max} + 1 \leq N_{s/r}$. This corresponds to the Nyquist theorem applied to circumferential mode.

In the previous sections, only aliasing of spinning modes due to a single source ring has been considered. However, modes have both spinning and radial orders which are coupled by an axial wavenumber, $\alpha_{mn} = \sqrt{1 - (\kappa_{nm}/k)^2}$. Modes could therefore be discriminated by their spinning order and axial wavenumber. If $|m_1| \neq |m_2|$, there is little possibility that $\alpha_{m_1 n}$ and $\alpha_{m_2 n}$ have same value since each κ_{mn} has distinct values.

Suppose $N_{s/r}$ is even and $N_{s/r} < 2m_{\max} + 1$, then two modes satisfying

$$\begin{aligned} m_1 &= +N_{s/r}/2, \\ m_2 &= -N_{s/r}/2 \end{aligned} \quad (23)$$

have same axial wavenumber

$$\alpha_{m_1 n} = \alpha_{m_2 n} = \sqrt{1 - (\kappa_{N_{s/r}/2n}/k)^2}. \quad (24)$$

Two modes are axially aliased, in addition to circumferential aliasing. This is the worst case for source reconstruction.

Suppose (m_1, m_2) is (even, odd) pair, then the condition $|m_1| \neq |m_2|$ is satisfied. Then two modes are generated independently by virtue of their different axial wavenumbers. This explains why the optimal value of $N_{s/r}$ is odd and less.

The effect of distance between source rings on the reconstruction accuracy of the ‘EEpM’ sound field is now investigated to identify the optimum ring separation distance for accurate mode synthesis. The wavelength in the axial direction is given by λ/α_{mn} , where λ is the free-space wavelength. It varies between λ at frequencies well above cut-on, to ∞ at the cut-off frequency ($\alpha_{mn} = 0$.) The standard deviation of the normalized energy per mode, $\sigma(\text{EpM}_{\text{norm}})$ versus $\Delta z/\lambda$ is plotted in Fig. 5 to examine the effect of ring distance for a number of frequencies between $ka = 10$ and 20.

In this simulation we assume $N_{s/r} = 19$ and $N_r = 8$, which are optimal for $ka = 20$. For ka less than 20, the assumed number of sources is greater than the number of optimal sources for a given ka to reconstruct the EEpM sound field and thus $\sigma(\text{EpM}_{\text{norm}})$ drops quickly for a small value of $\Delta z/\lambda$. For $ka = 20$, the standard deviation of energy per mode drops continually, reaching its smallest value when $\Delta z/\lambda = 1$. The standard deviation of normalized energy per mode versus ring distance for various ka is plotted in Fig. 3b. The optimal ring distance to generate an accurate broadband sound field with an upper frequency limit of $ka = 20$ is predicted to be $\Delta z = 0.3m$ which is the free-space wavelength at the highest wavenumber of $ka = 20$ and $a = 1m$.

3.2. Optimal shaping filters for the generation of $EEpM$

The number of shaping filters required to drive N_{tot} sources is N_{tot}^2 . At $ka = 20$, for example, the number of sources is 152, comprising 19 and eight sources per ring. The corresponding number of shaping filters is $152^2=23,000$. Some examples of shaping filters and source strength power spectra are presented in Figs. 6 and 7 plotted over a non-dimensional frequency range of $1 < ka < 20$. Here the ratio of source ring separation distance and duct radius is $\Delta z/a = 0.3$.

Although the total sound power in a unit frequency band stays constant, the magnitude of the source strength spectrum is found to increase with increasing frequency as $(ka)^4$ since the number of propagating modes increase with frequency as $(ka)^2$. For example, S_{qq11} is the source strength at $z = 0, \varphi = 0$. From Eq. (11), note that S_{aa} is diagonal matrix, S_{qq11} is given by

$$S_{qq11} = \sum_{l=1}^K g_{1l} S_{aall} g_{1l} \tag{25}$$

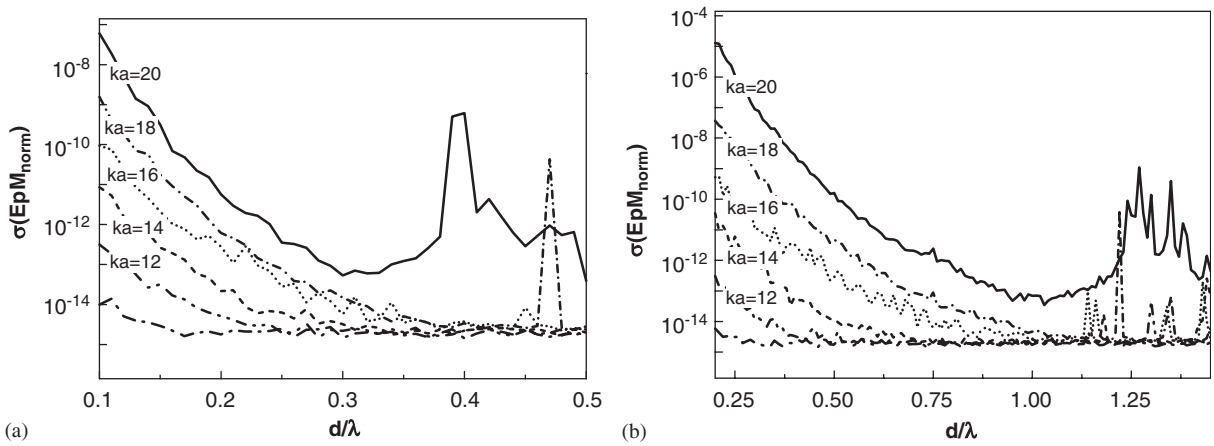


Fig. 5. Effect of ring distance is evaluated compared with wavelength and distance for $ka = 20, 18, 16, 14, 12, 10,$ and 8 . $N_{s/r} = 19, N_r = 8, a = 1$ m. (a) Standard deviation of normalized energy per mode versus d/λ . (b) Standard deviation of normalized energy per mode versus distance.

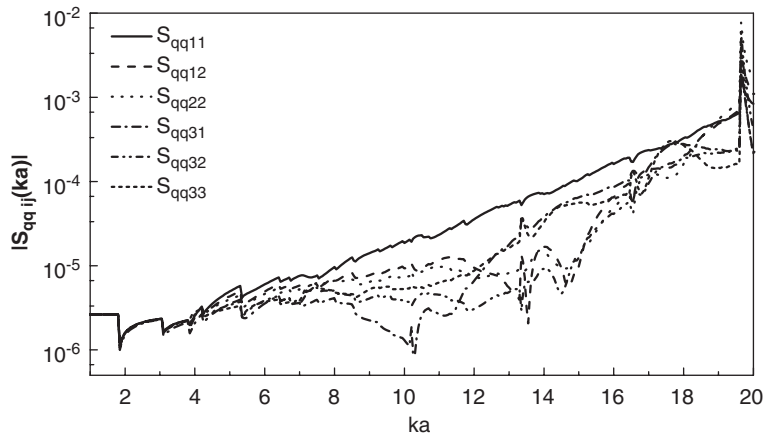


Fig. 6. Several examples of magnitude of source strength spectrum are drawn. Source strength spectrum which generates equal energy per mode and incoherent broadband sound field with 19 sources per source rings and eight source rings with ring distance of 0.3 m and radius of 1 m.

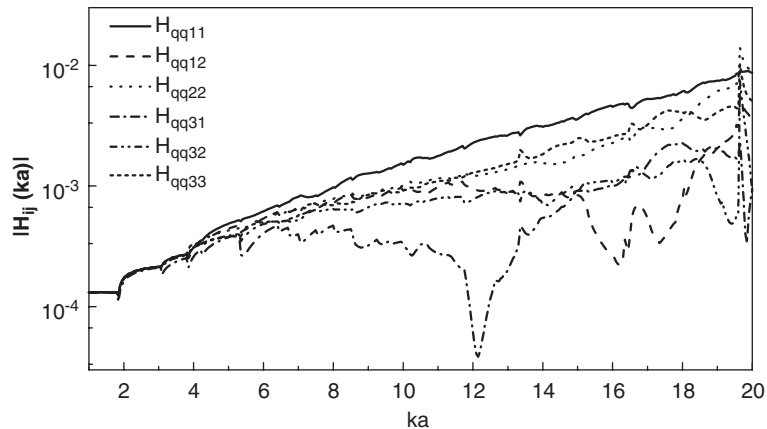


Fig. 7. Several examples of shaping filter spectrum are drawn. Shaping filters could be driven by white noises to source strength signal which generates equal energy per mode and incoherent broadband sound field with 19 sources per source rings and eight source rings with ring distance of 0.3 m and radius of 1 m.

in which S_{all} denotes the l th diagonal element in the matrix S_{aa} and K is the number of propagation modes. The terms g_{1l} , g_{l1} , and S_{aa11} at $z = 0$ are real numbers and K is proportional to $(ka)^2$. Thus magnitude of S_{qq11} is approximately proportional to $(ka)^4$.

The sudden drop in the source strength spectra at low frequencies in Fig. 6 coincides with the modal cut-on frequencies ($\alpha_{mm} \simeq 0$). Close to the cut-on frequencies, the mode is almost a two-dimensional standing wave which requires comparatively little source strength to drive it in a hard-wall duct [5]. The required time-averaged sound power of modes close to the cut-on frequency can be readily deduced from Eq. (4). In the high-frequency region, cut-on effects are masked by numerous other well cut-on modes. Fig. 7 shows the magnitude of the shaping filter calculated using Eq. (18). The behavior of the shaping filter spectrum and the source strength spectrum is found to be similar.

4. Conclusion

A technique for generating broadband sound fields with EEPM and modal incoherence characteristics in a hard-walled duct with wall-mounted source is described. This method for generating ‘EEPM’ sound field could be used for broadband sound field with different modal characteristics or different kind of source distribution.

The optimal number of sources per ring and the optimal numbers of source ring for circular duct are investigated. It is shown from considerations of the aliasing between modes in circular duct that the optimal numbers of sources per ring are always odd and less than the number of total possible total circumferential modes. The number of source rings is shown to be comparable to the possible number of radial modes. The effect of source ring distance is examined by considering the standard deviation of the energy per mode. The result shows that the optimal ring distance for broadband sound field generation is related to the wavelength at the highest frequency of interest.

Examples of the shaping filters and source spectrum are given as functions of non-dimensional frequency up to $ka = 20$ with 19 sources per ring and eight source rings. The shaping filters are acquired from decomposition of the optimal source spectrum matrix. The shaping filters driven by white noise signals could be used to produce source strength signals for wall-mounted sources, which generate EEPM broadband sound field with uncorrelated mode amplitudes.

Acknowledgements

This work is supported by International Cooperation Research Program of Ministry of Science and Technology and the Brain Korea 21 Project.

References

- [1] E.J. Rice, Multimodal far-field acoustic radiation pattern using mode cutoff ratio, *American Institute of Aeronautics and Astronautics Journal* 16 (1978) 906–991.
- [2] P. Joseph, C.L. Morfey, Multi-mode radiation from an unflanged, semi-infinite circular duct, *Journal of the Acoustical Society of America* 105 (5) (1999) 2590–2600.
- [3] A. Snakowska, On the principle of equipartition of energy in the sound field inside and outside a circular duct, *Acustica* 79 (1993) 155–160.
- [4] P. Joseph, C.L. Morfey, C.R. Lewis, Multi-mode sound transmission in ducts with flow, *Journal of the Acoustical Society of America* 264 (2003) 523–544.
- [5] P.E. Doak, Excitation, transmission and radiation of sound from source distributions in hard-walled ducts of finite length (I): the effects of duct cross-section geometry and source distribution space-time pattern, *Journal of Sound and Vibration* 31 (1973) 1–72.